

# Grassy ELM regime at low pedestal collisionality in high-power tokamak plasma

Y.F. Wang<sup>1</sup>, H.Q. Wang<sup>2</sup>, **G.S. Xu<sup>1\*</sup>**, G.Z. Jia<sup>1</sup>, F. Turco<sup>3</sup>, C.C. Petty<sup>2</sup>, J.L. Chen<sup>1</sup>, N. Yan<sup>1</sup>, Q.Q. Yang<sup>1</sup>, L. Wang<sup>1</sup>, R. Chen<sup>1</sup>, G.H. Hu<sup>1</sup>, T.H. Osborne<sup>2</sup>, P.B. Snyder<sup>2</sup>, A.M. Garofalo<sup>2</sup>, X.Z. Gong<sup>1</sup>, J.P. Qian<sup>1</sup>, G.Q. Li<sup>1</sup>, H.Y. Guo<sup>2</sup> and B.N. Wan<sup>1</sup>



<sup>1</sup>Institute of Plasma Physics, Hefei Institutes of Physical Science, Chinese Academy of Sciences, Hefei 230031, People's Republic of China

<sup>2</sup>General Atomics, PO Box 85608, San Diego, CA 92186-5608, United States of America

<sup>3</sup>Columbia University, 2960 Broadway, New York, NY 10027-6900, United States of America

\*Email: [gsxu@ipp.ac.cn](mailto:gsxu@ipp.ac.cn)

10<sup>th</sup> US-PRC Magnetic Fusion Collaboration Workshop, Mar 22-26, 2021

# Outline

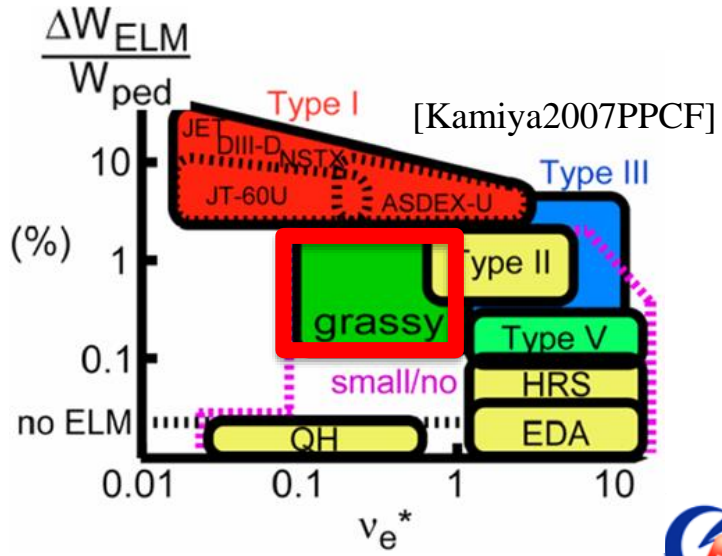
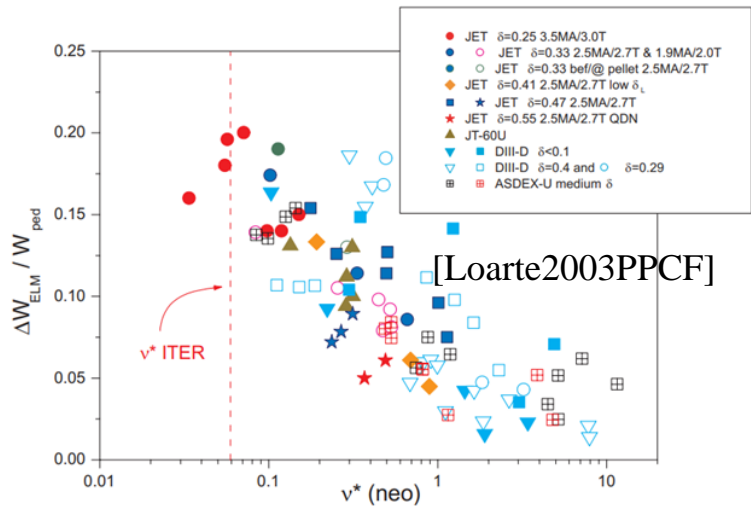
- **1. Motivation**
- **2. Intrinsic grassy ELM regime in DIII-D**
- **3. Prediction of access to grassy ELM regime in CFETR**
- **4. Summary**

# Outline

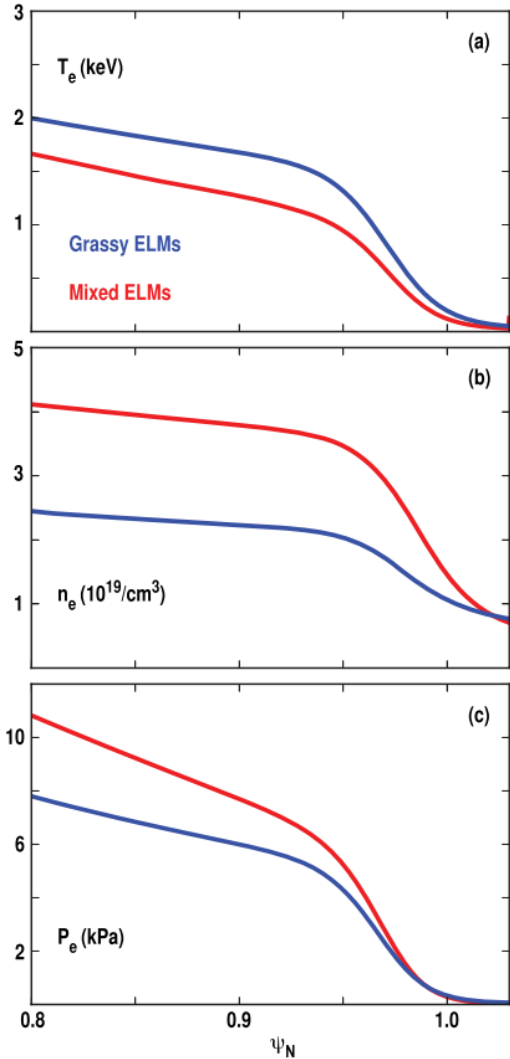
- **1. Motivation**
- **2. Intrinsic grassy ELM regime in DIII-D**
- **3. Prediction of access to grassy ELM regime in CFETR**
- **4. Summary**

# The grassy ELM regime offers a potential candidate for the operation of future fusion reactors

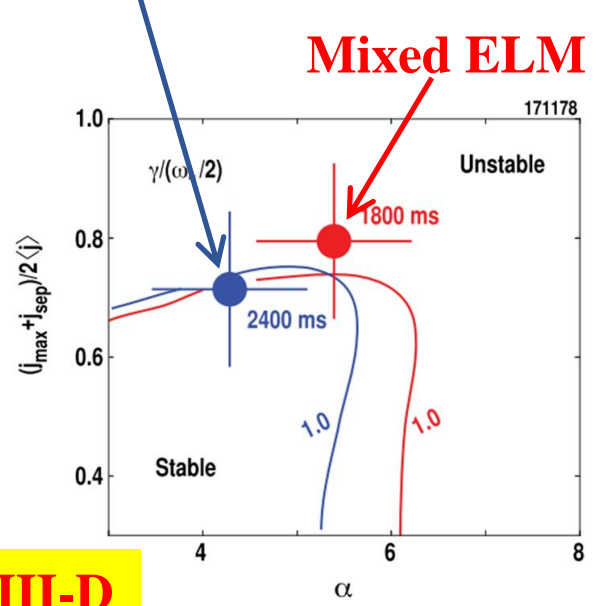
- Large ELMs at low  $v^*$  induces intolerable heat load for reactors.
- Grassy ELM regime is potentially accessible at relatively low pedestal collisionality and compatible with high- $\beta_p$  steady-state operational scenarios  
➔ CFETR
- High  $\beta_p$ , high  $q_{95}$  and high plasma shaping facilitate access to grassy ELMs.
- Further study is required to understand the physics of the grassy ELM regime.



# The importance of pedestal density profile has been highlighted in recent grassy ELM studies

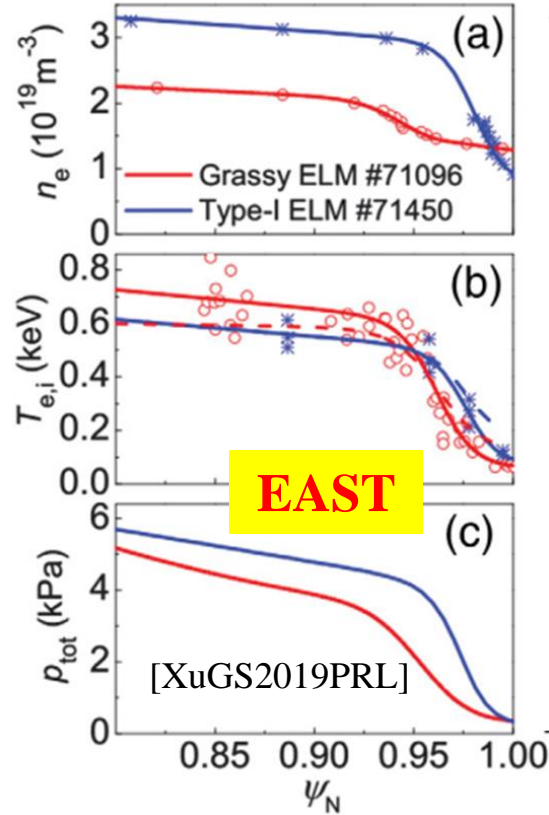


## Grassy ELM (w. RMP)



**DIID-D**

[Nazikian2018NF]



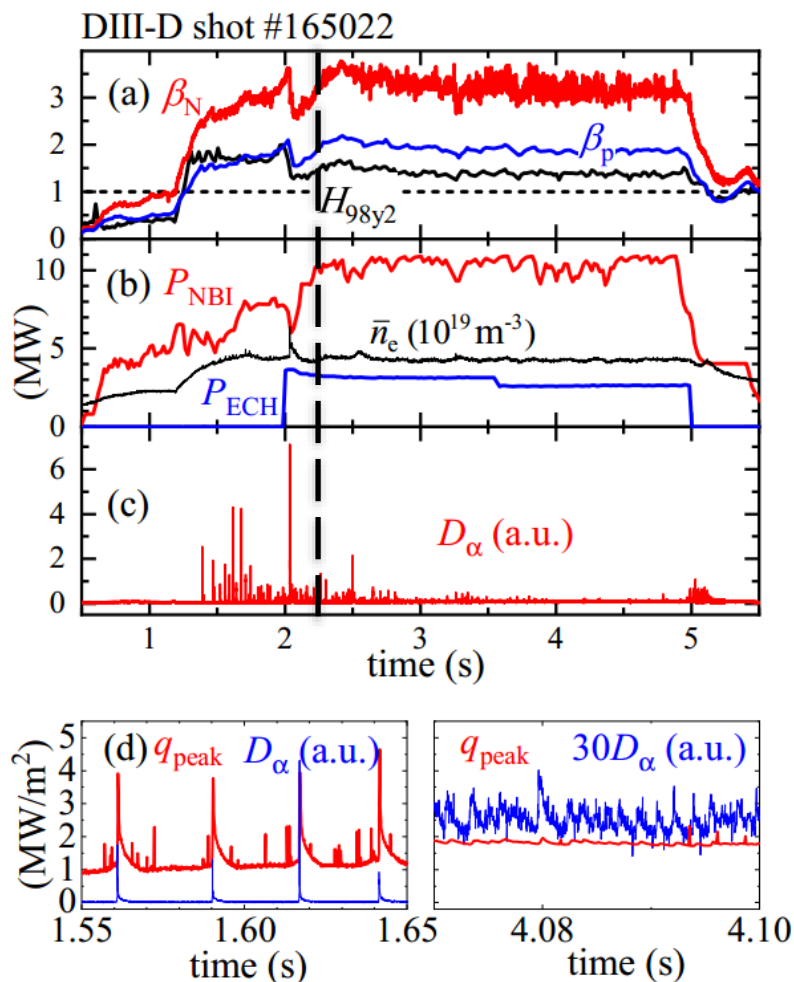
**EAST**

- $\nabla n_{e,\text{ped}}$  in grassy ELM regime appears to be much smaller than that in large ELM regime.
- For the grassy ELM regime, the operational point is located near the peeling boundary.

# Outline

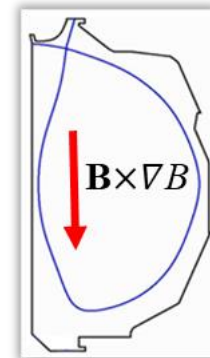
- 1. Motivation
- 2. Intrinsic grassy ELM regime in DIII-D
- 3. Prediction of access to grassy ELM regime in CFETR
- 4. Summary

# Giant ELMs appear to be spontaneously mitigated and replaced by grassy ELMs as heating power increases



➤ Giant ELMs are replaced by grassy ELMs.

- DND configuration with unfavorable  $B_T$
- $q_{95} \sim 6.2$ ,  $n_e/n_{GW} \sim 0.53$ ,  $f_{BS} \sim 50\%$ .
- $P_{\text{inj}}$  increases from 6MW to 13MW.



➤  $q_{\text{peak-ELM}}$  is reduced by >90%.

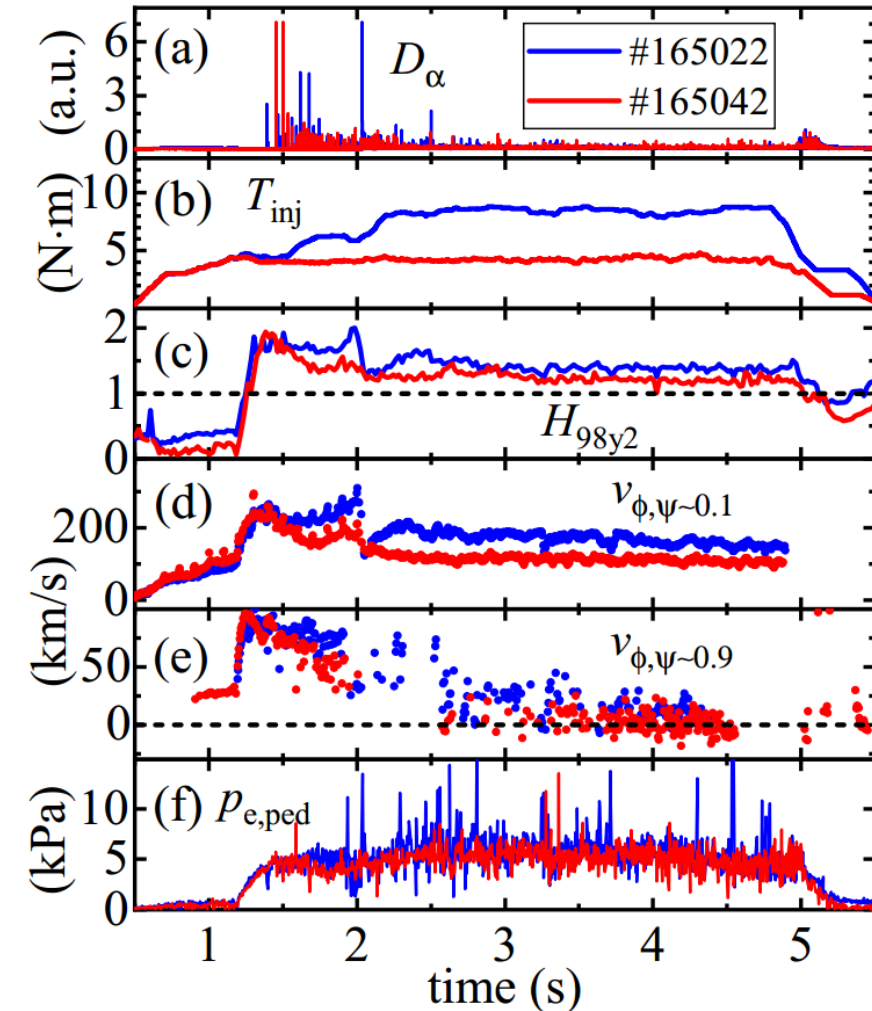
➤ No RMP is intentionally applied.

➤ Good energy confinement:  $H_{98y2} \sim 1.4$ ,  $\beta_p \sim 1.9$ ,  $\beta_N \sim 3.2$

➤ ITER-relevant low  $v_{e,\text{ped}}^* \sim 0.15$  is achieved

< 1MW/m<sup>2</sup>

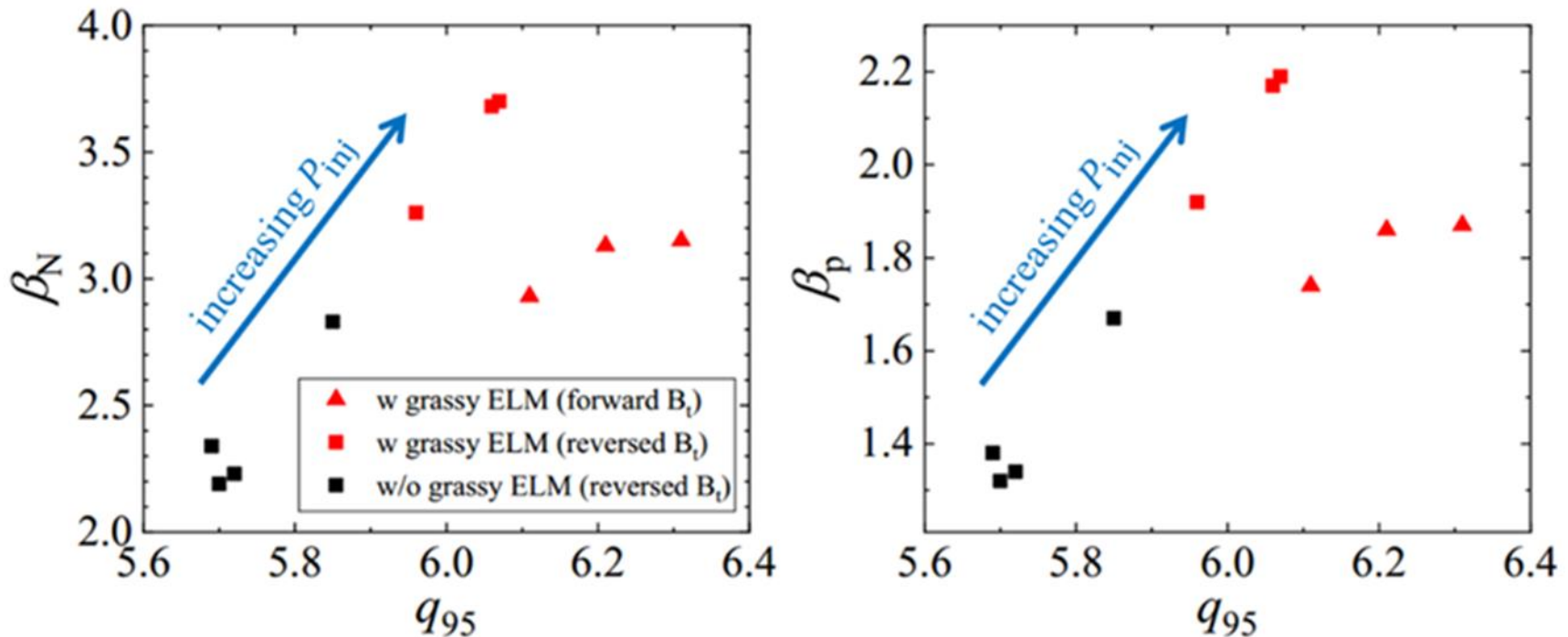
# Even at reduced torque, high confinement and high pedestal are still obtained in the grassy ELM regime



- The grassy ELM regime has been achieved within a certain range of neutral beam torque.
- Similar discharge conditions except  $T_{NBI} \sim 8.6/4.4$  Nm
- Higher  $H_{98y2}$  at higher  $T_{NBI}$ 
  - Higher core rotation at higher  $T_{NBI}$
  - Small edge rotation change
- Similar pressure pedestal structure



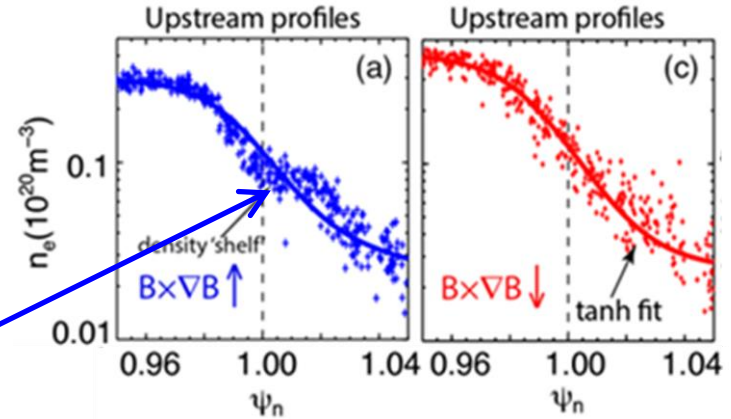
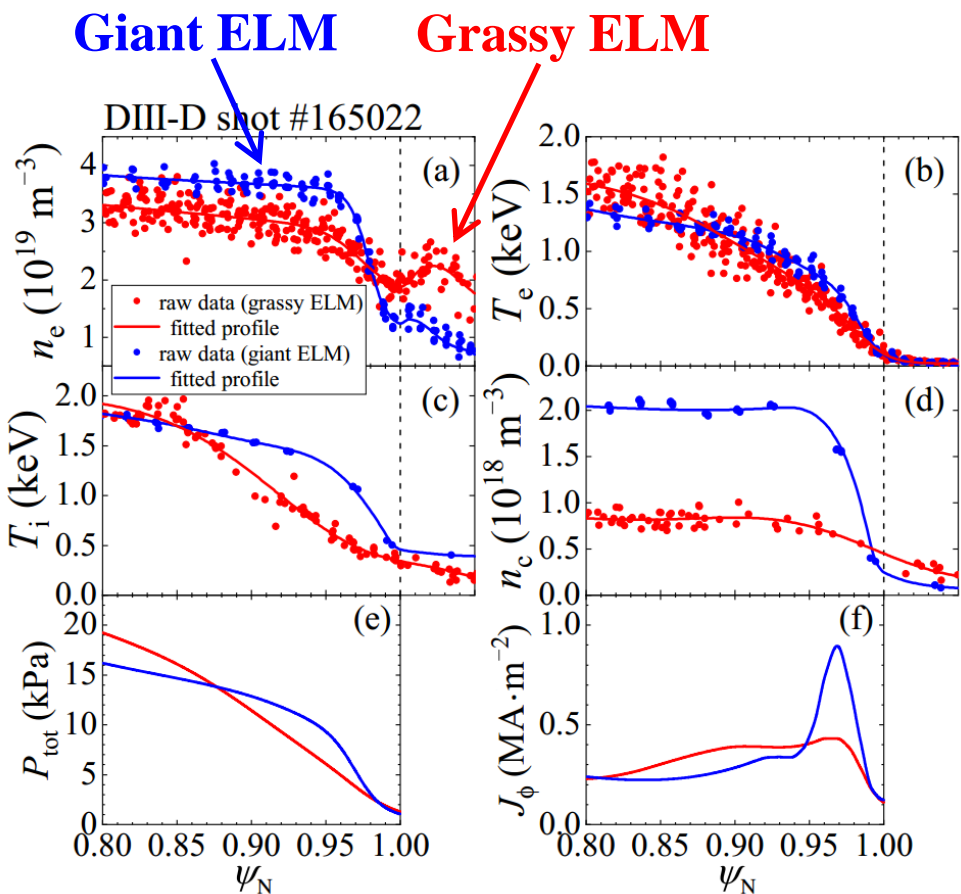
# Higher heating power appears to facilitate access to the grassy ELM regime



- Compare discharges with similar  $I_p$ ,  $B_T$  (unfav.),  $n_e$  and plasma shape
- Divertor geometry effect may be not a dominant factor to enter this regime.

# Density pedestal in the grassy ELM regime is characterized by lower density gradient and higher $n_{e,sep}/n_{e,ped}$

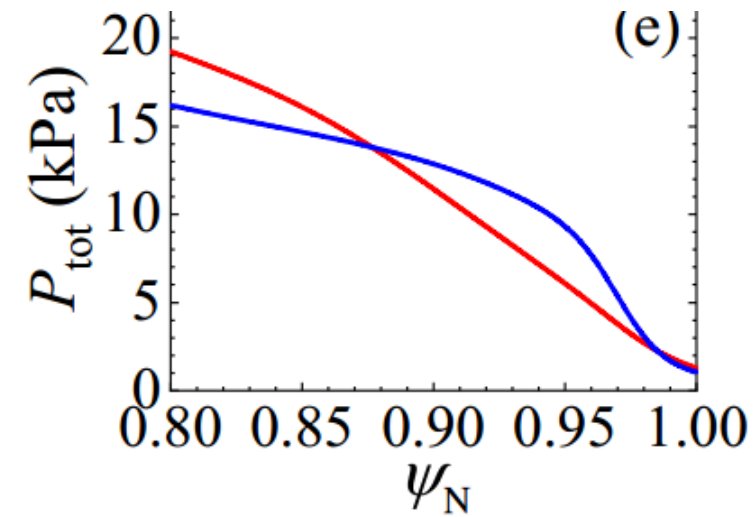
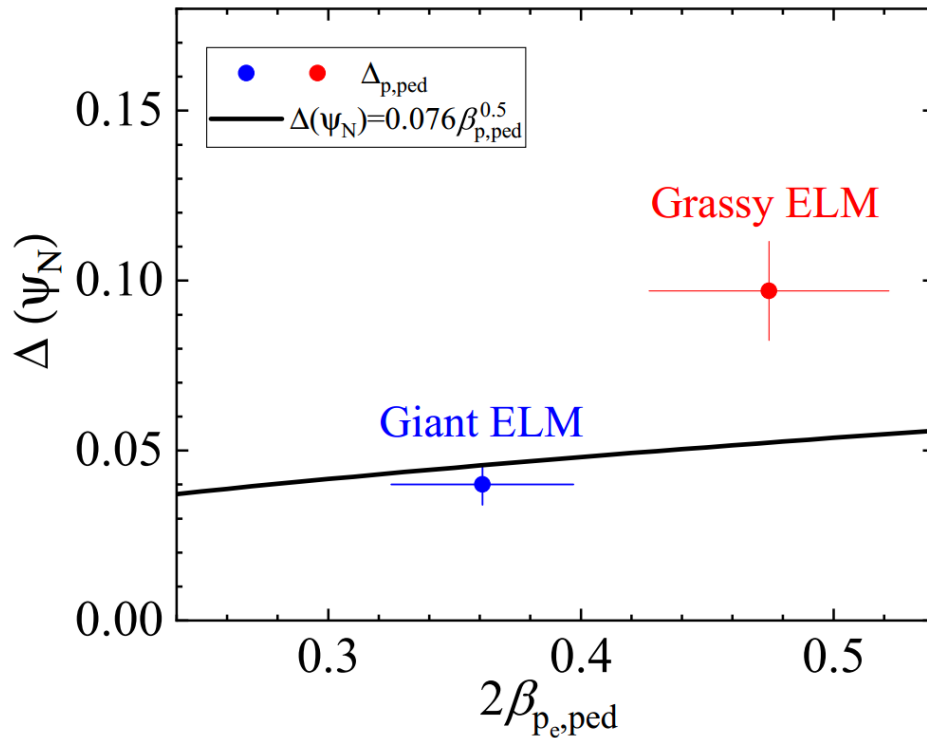
- $n_{e,sep}/n_{e,ped}$  : **35%** vs. **65%** (before vs. **after** raising heating power) with similar line-averaged density
- Both Te and Ti pedestals appear to become wider and flatter.
- The carbon impurity density is significantly reduced.
- Kinetic equilibria are reconstructed.



Density shelf exists under unfavorable  $B_T$

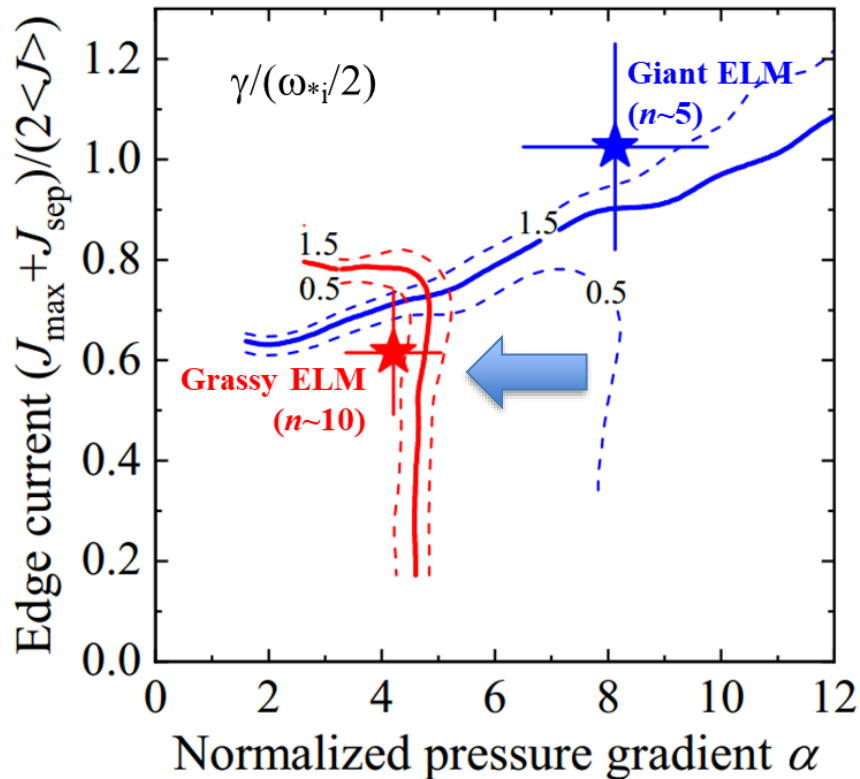
[WangHQ2020PRL]

# Pedestal width in the grassy ELM regime exceeds the EPED1.0 model prediction by more than 50%



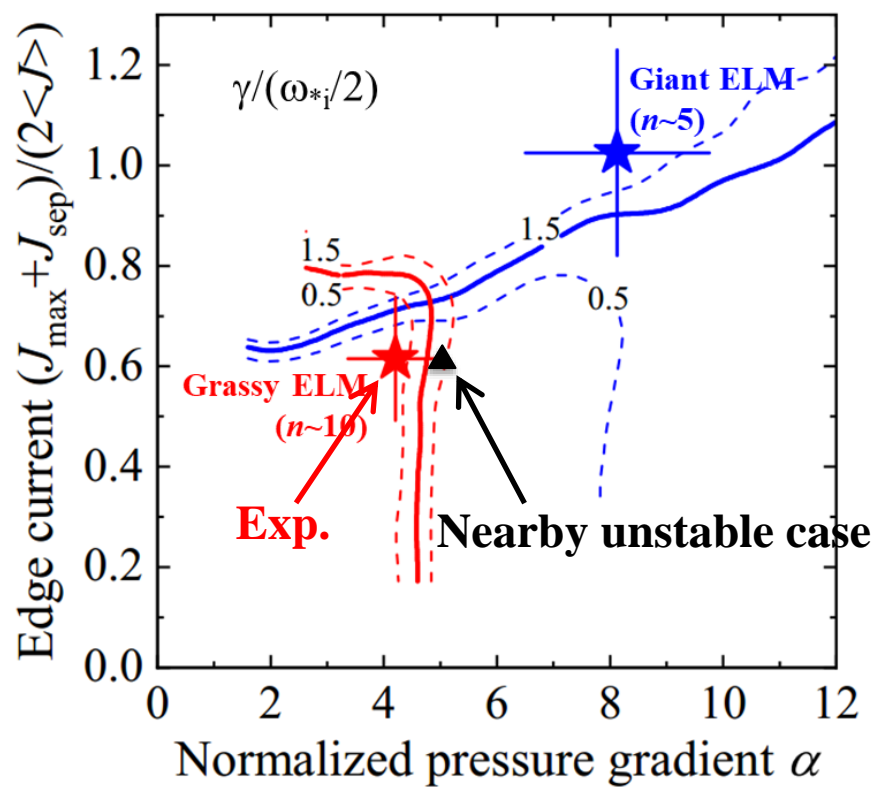
- Pedestal width in giant ELM regime is consistent with that predicted by the EPED1.0 model.
- The wide pedestal in grassy ELM regime leads to a high pressure at the pedestal top even though there is a low pedestal pressure gradient. This explains why good energy confinement is achieved in the grassy ELM regime.

# The operational point in the grassy ELM regime is located near the ballooning boundary



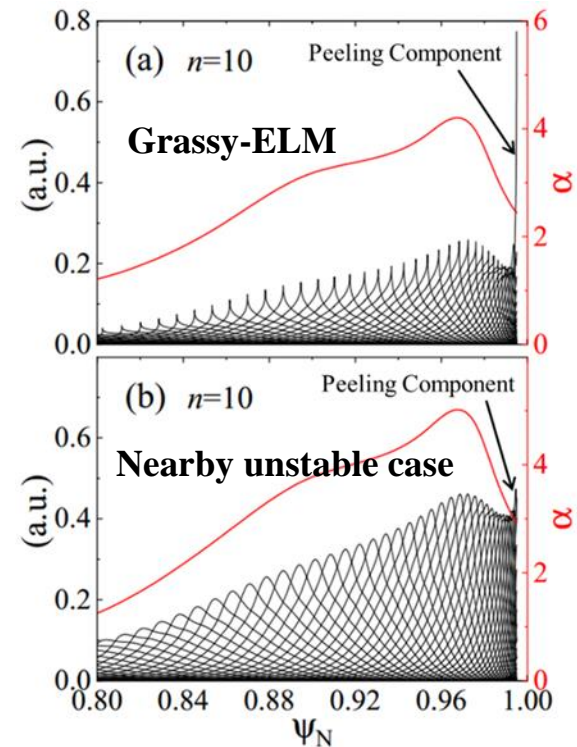
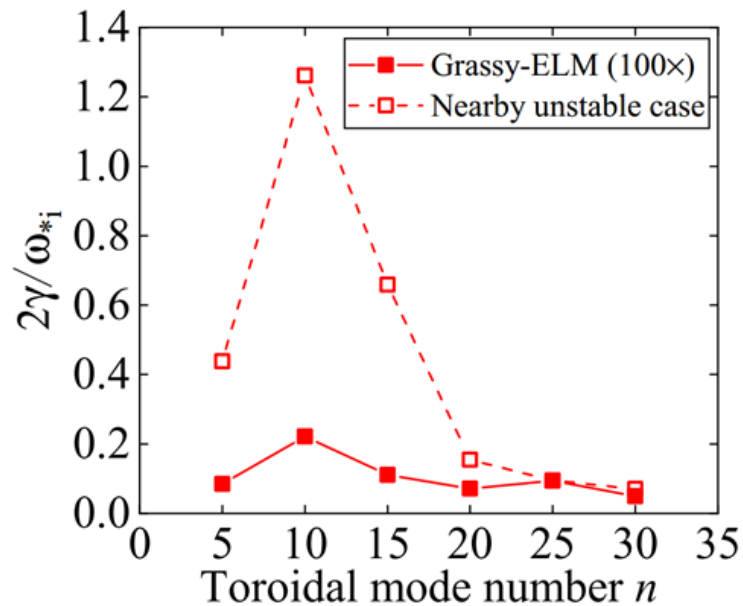
- The values of  $\alpha$  and  $J_N$  are both smaller in the grassy ELM regime.
- The ballooning boundary retreat significantly in the grassy ELM regime.
- The pedestal stability against low-n kink/peeling modes is improved after access to the grassy ELM regime.

# The operational point in the grassy ELM regime is located near the ballooning boundary



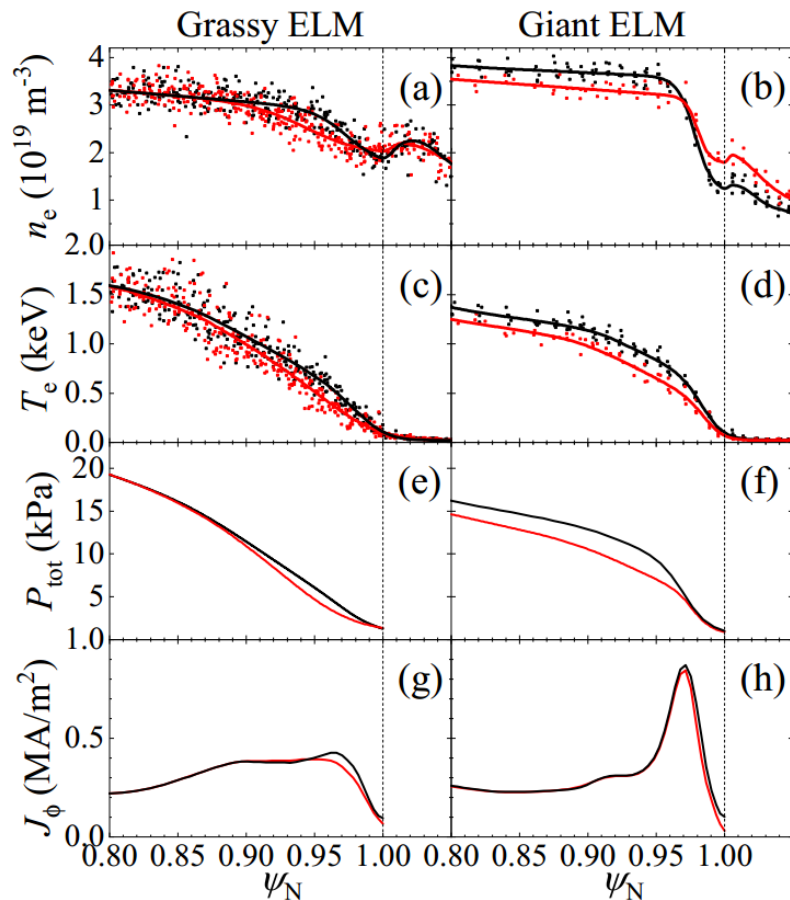
- The values of  $\alpha$  and  $J_N$  are both smaller in the grassy ELM regime.
- The ballooning boundary shrinks significantly in the grassy ELM regime.
- The pedestal stability against low-n kink/peeling modes is improved after access to the grassy ELM regime.

# The ballooning component of the most unstable mode structure becomes stronger in the nearby unstable case

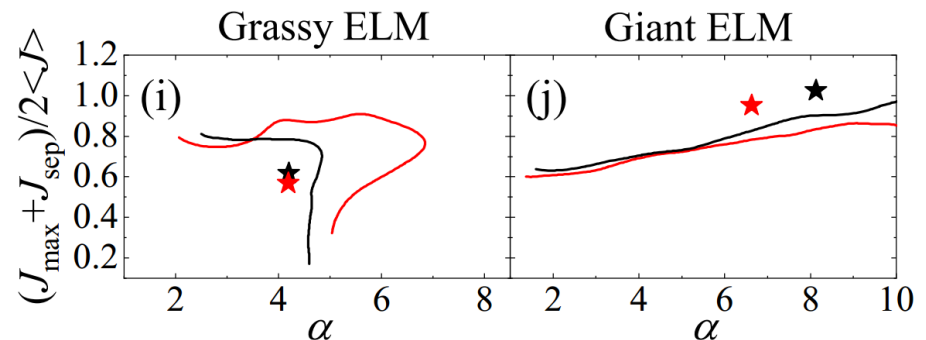


- The grassy ELMs are most likely triggered by intermediate- $n$  ( $n \sim 10$ ) PBMs.
- The ballooning component of the most unstable mode structure becomes stronger while the peeling component becomes weaker in the nearby unstable case, suggesting the dominant unstable modes are the ballooning modes

# During grassy ELM crash, the ballooning boundary expands and helps to stop further pedestal collapse



- Comparison of profiles before (black) and after (red) ELM crashes
- Giant ELMs induce large crashes
  - Move along the peeling boundary
- During grassy ELM crashes, the ballooning boundary expands due to an initial radially localized small pedestal collapse.



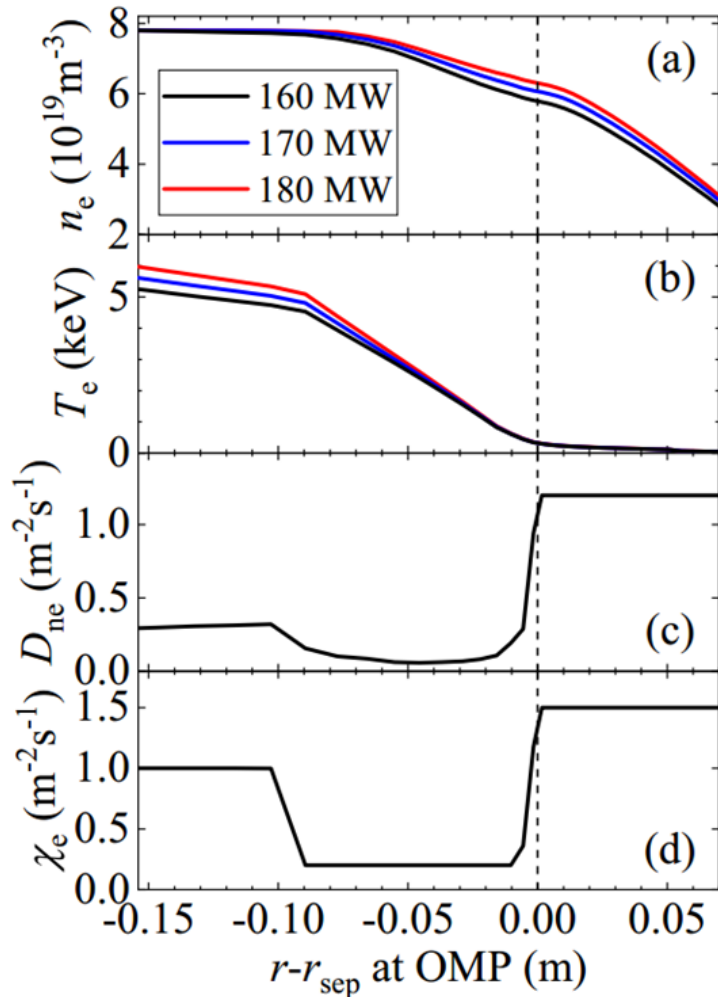
# Outline

- 1. Motivation
- 2. Intrinsic grassy ELM regime in DIII-D
- 3. Prediction of access to grassy ELM regime in CFETR
- 4. Summary



# Higher heating power is beneficial to formation of higher separatrix density

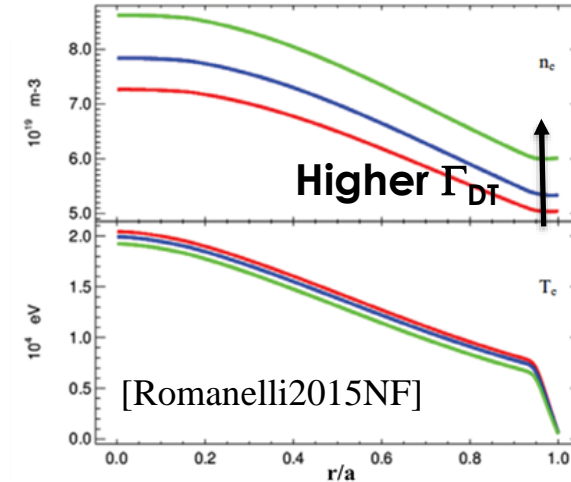
## □ Scan input power $P_{input}$



## SOLPS-ITER code simulation domain



High  $n_{e,sep}$  similar to SOLPS simulations of ITER plasmas →

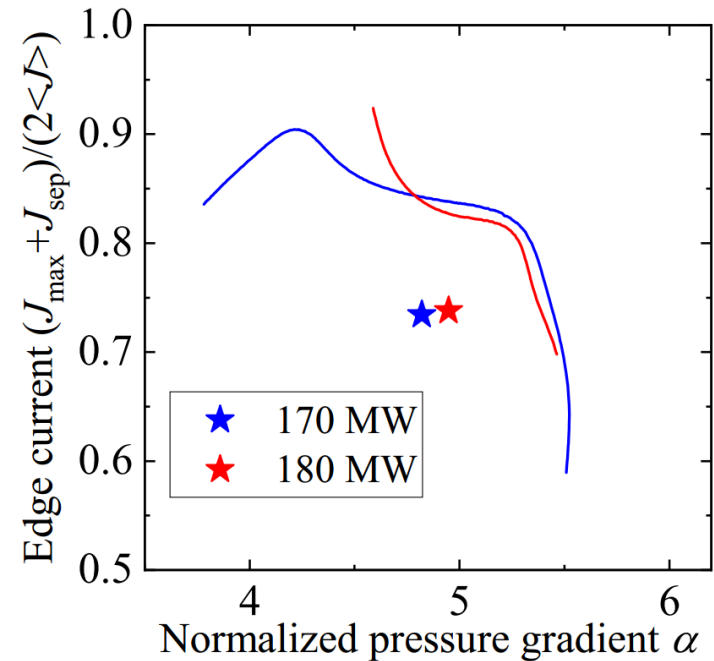
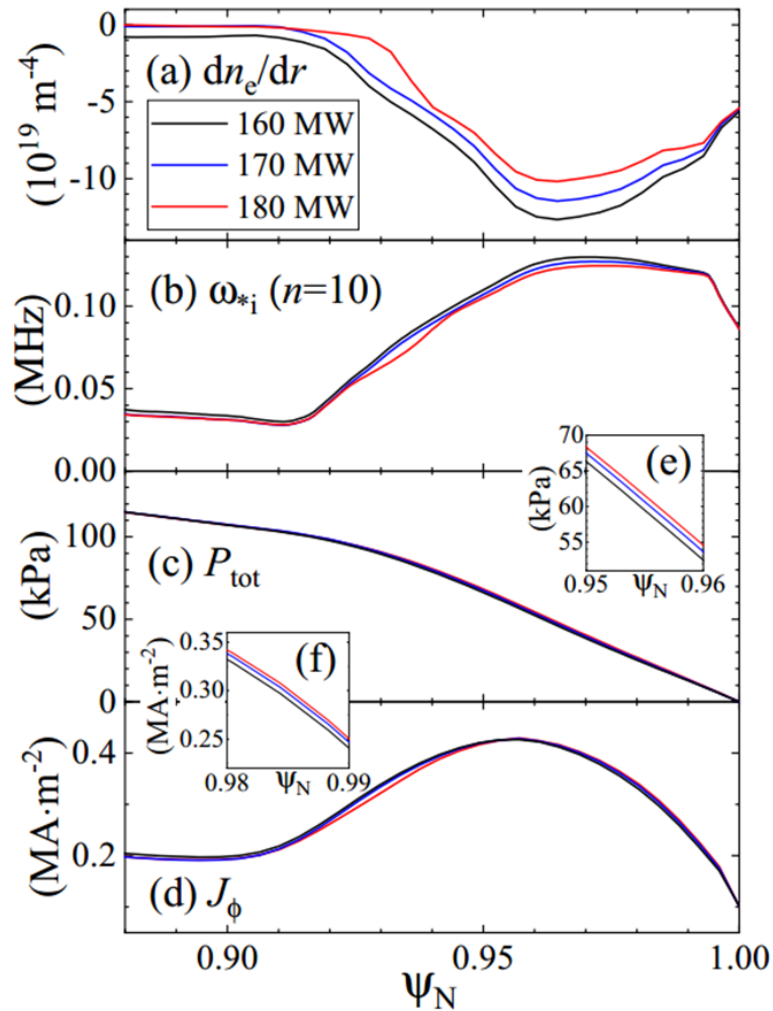


- The separatrix electron density increases with  $P_{input}$ .

$$n_{e,sep} = \frac{1.1 \times 10^{15} q_{||}^{5/7}}{L_{||}^{2/7} T_{e,div}^{1/2}} \left( \frac{1 - f_{rad}}{1 - f_{mom}} \right)$$

- The increased  $P_{input}$  also enhances the electron temperature at the pedestal top.
- The separatrix electron temperature changes very little.

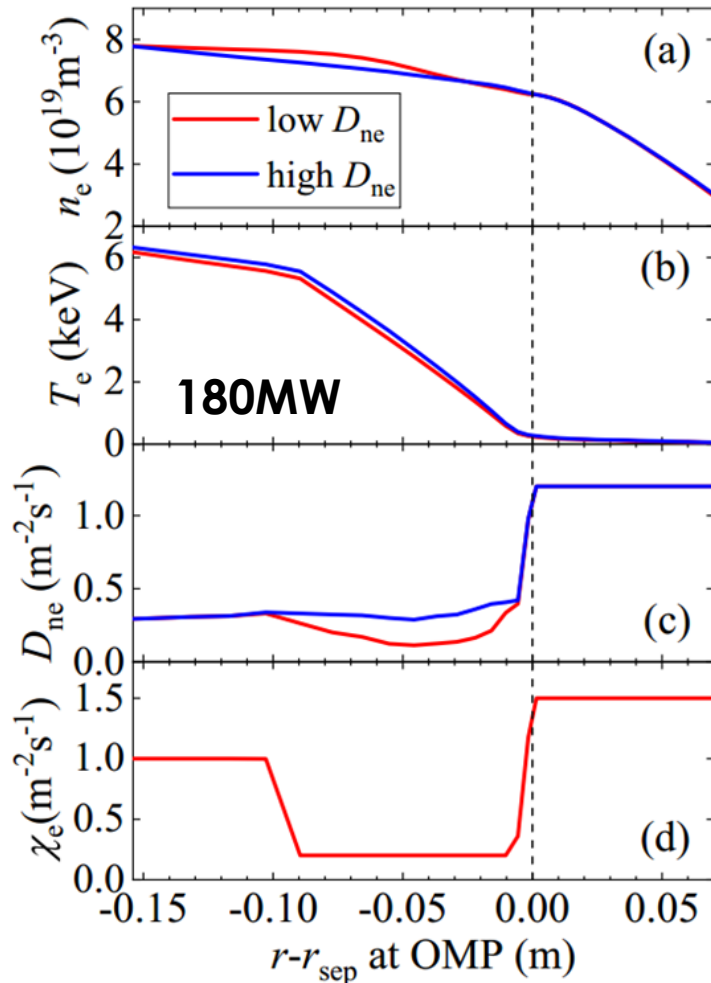
# Higher separatrix density would help to destabilize ballooning modes and facilitate the access to the grassy ELM regime



- Pedestal stability analysis with  $n_e$  profiles produced in SOLPS simulations
- With higher heating power and thus higher separatrix density, the operational point moves closer to the ballooning boundary.

# Separatrix density might be insensitive to the pedestal electron diffusivity

## □ Modify pedestal electron diffusivity $D_{ne}$



- The electron density and temperature at the pedestal top slightly change.
- The electron density and temperature at the pedestal foot and in the SOL changes very little.
- Suggest that the separatrix density and temperature is insensitive to the pedestal diffusivity and they are mainly determined by the divertor and SOL physics.
- Confirm our argument that this kind of density profile very likely appear in future fusion reactors.

# Outline

- 1. Motivation
- 2. Intrinsic grassy ELM regime in DIII-D
- 3. Prediction of access to grassy ELM regime in CFETR
- 4. Summary

# Summary

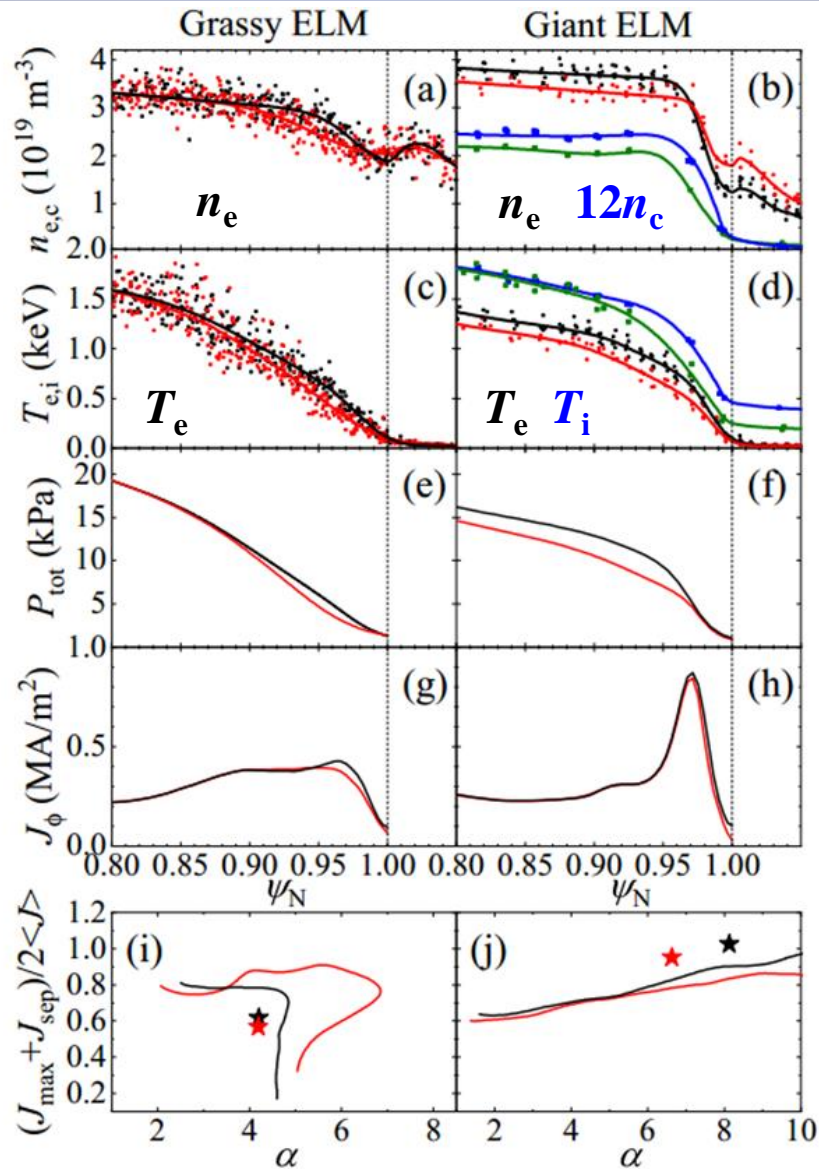
- **A naturally spontaneous grassy ELM regime has been achieved in high-power ( $P_{inj} > 13\text{MW}$ ) hybrid scenario in DIII-D.**
  - $v_{ped}^* \sim 0.15$ ,  $H_{98y2} \sim 1.4$ ,  $\beta_N \sim 3.2$ , low ELM peak heat flux  $< 1\text{MW/m}^2$
- **The low pedestal density gradient and high  $n_{e,sep}/n_{e,ped}$  help stabilize the peeling-ballooning modes and destabilize ballooning modes.**
  - The operation point locates near the ballooning boundary.
- **SOLPS simulation of CFETR plasmas suggests that the density pedestal could be very flat with high  $n_{e,sep}$ , especially at high heating power, which is considered to facilitate the access to the grassy ELM regime.**
  - The grassy ELM regime is potentially more easily accessible in ITER, CFETR and other future large fusion devices.

# Thank you!

# Backup

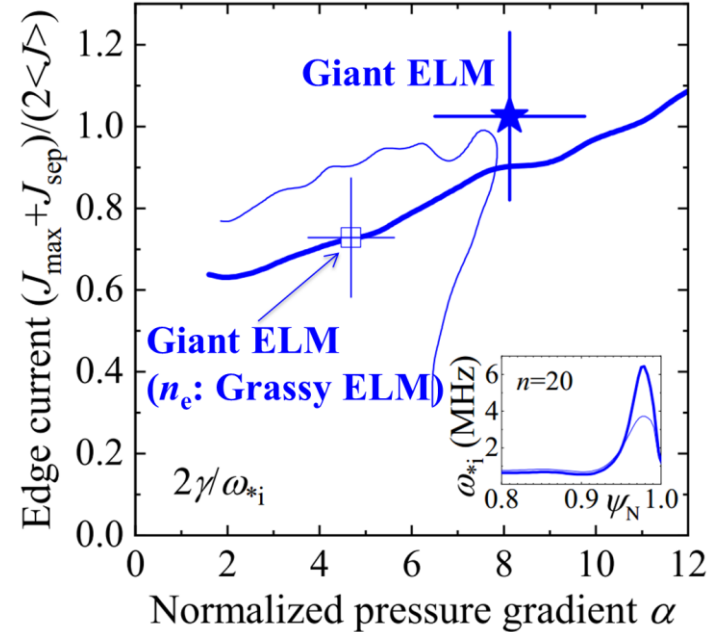
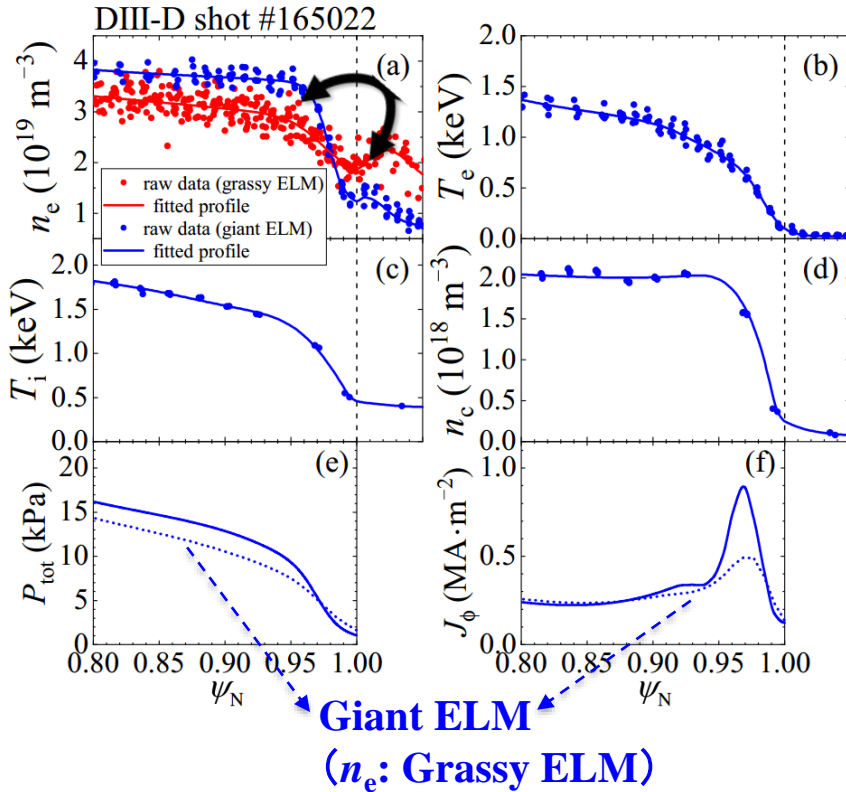
Table 1. The shot numbers involved are listed as well as basic discharge parameters obtained by taking 500 ms average of corresponding signals on the  $\beta_N$  flattop phase of each shot. The plasma current  $I_p$  is 0.98 MA in all shots. The plasmas are all in the near-double null divertor (DND) configuration with unfavorable toroidal magnetic field  $B_t$  direction (Negative/positive represents reversed/forward  $B_t$ ).

shot	$B_t$ /T	$q_{95}$	$\beta_p$	$l_i$	$\bar{n}_c / 10^{19} \text{m}^{-3}$	$P_{inj}$ /MW	$T_{inj}$ /N·m	$H_{98y2}$	w or w/o grassy ELM
165022	-1.98	6.21	1.86	0.80	4.26	13.0	8.58	1.38	w
165024	-1.98	6.31	1.87	0.80	4.27	13.7	8.45	1.36	w
165042	-1.98	6.11	1.74	0.82	4.24	14.3	4.37	1.19	w
170272	1.97	5.96	1.92	0.84	3.83	14.6	5.49	1.24	w
170317	1.97	6.07	2.19	0.81	4.29	14.6	9.15	1.55	w
170325	1.97	6.06	2.17	0.82	4.30	14.6	9.15	1.52	w
170333	1.97	5.85	1.67	0.87	3.93	13.0	3.12	1.19	w/o
170335	1.97	5.69	1.38	0.94	4.30	11.5	0.66	1.05	w/o
170336	1.97	5.72	1.34	0.90	4.26	9.6	0.78	1.06	w/o
170340	1.97	5.70	1.32	0.90	4.32	9.2	2.19	1.03	w/o



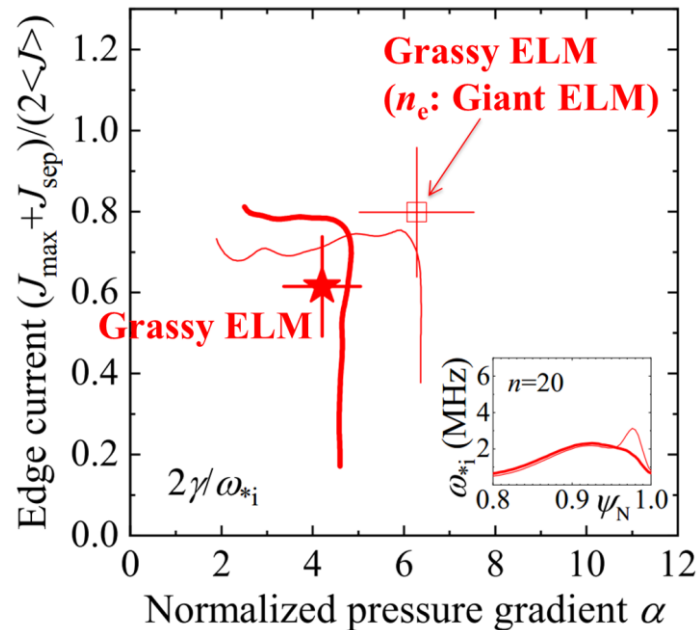
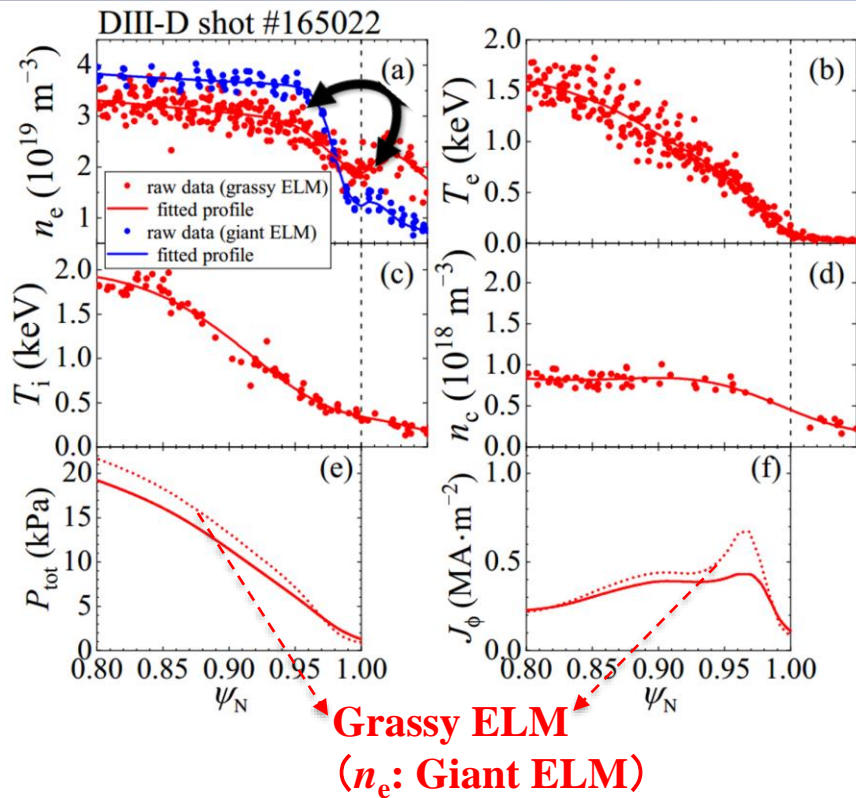


# The narrowing of the ballooning boundary mainly attributes to lower $\omega_{*i}$ in the pedestal region



- The  $n_e$  profiles are exchanged numerically in the both cases.
- With  $n_e$  from the grassy ELM case,  $\alpha$  and  $J_N$  of the operational point both decrease and the ballooning boundary narrows because of lower  $\omega_{*i}$ .
  - ion diamagnetic frequency  $\omega_{*i} \sim \nabla p_e / n_e$

# The low density gradient and high $n_{e,sep}/n_{e,ped}$ help stabilize the peeling-ballooning modes and narrow ballooning boundary



- With  $n_e$  from the giant ELM case,  $\alpha$  and  $J_N$  of the operational point both increase and the ballooning boundary expands.
- The  $n_e$  pedestal in the grassy ELM regime helps to stabilize PBMs with lower pressure pedestal gradient and narrow ballooning boundary with lower  $\omega_{*i}$ .